Generation and Detection of Quantum Turbulence in Superfluid ^{3}He-*B*

S. N. Fisher, A. J. Hale, A. M. Guénault, and G. R. Pickett
Department of Physics, Lancaster University, Lancaster LA1 4YB, United Kingdom
(Received 9 August 2000)

We describe the first direct observations of turbulence in superfluid ^{3}He-*B*. The turbulence is generated by a vibrating-wire resonator driven at velocities exceeding the pair-breaking critical velocity. It is detected by the resulting decrease in the thermal damping on a neighboring "detector" vibrating-wire resonator. The superfluid flow field associated with the turbulence Andreev reflects thermal quasiparticle excitations, effectively screening the detector wire, resulting in a decrease in the thermal damping.

DOI: 10.1103/PhysRevLett.86.244 PACS numbers: 67.40.Vs, 67.55.Hc, 67.57.De

Superfluid turbulence has been studied for many years in superfluid ^{4}He (see, for example, Stalp *et al.* [1]). In superfluid ^{3}He turbulence has been indirectly inferred [2,3], but direct studies of vortices have previously been made only in rotating cryostats [4] where vortex lattices can be studied with NMR techniques. Superfluid turbulence in ^{4}He is easily generated, leading to the low critical velocities observed in flow experiments. In contrast, the critical velocities observed in superfluid ^{3}He-*B* occur at velocities approaching the Landau criterion for pair breaking [5]. However, once a tangle of vortices has been established in superfluid ^{3}He at the lowest temperatures, we can observe the turbulence in real time via the flow barrier it presents to the long range propagation of quasiparticles in the fluid. The flow changes the properties of the quasiparticle gas sufficiently for us to infer the behavior of the vortex tangle. We therefore present here the first observations of turbulence in superfluid ^{3}He.

The experiments are performed in a Lancaster-style nested nuclear cooling stage which also forms the experimental cell [6]. The outer cell contains sintered silver copper plate refrigerant which cools the contained liquid to a temperature below $0.15T_c$. The outer cell acts as a thermal guard reducing heat leaks into the inner cell which contains ~100 0.1 mm thick sintered silver copper plates. Two vibrating wire resonators (VWRs) are located in a volume cut from the inner cell shown in the inset in Fig. 2A. Each VWR is formed from a NbTi filament bent into an approximately semicircular shape with a diameter of 3 mm. The two wires are aligned back to back and spaced 1 mm apart. The two VWRs are designated the "generator" and the "detector" wire. The generator wire is formed of a single 13 μm filament, while the detector wire is a single 4.5 μm filament. The cell is demagnetized to a field of 68 mT which cools the superfluid *B* phase in the inner cell to a base temperature below $0.11T_c$.

In an ambient magnetic field, an ac current through the VWR loop causes it to oscillate from the Lorentz force. The moving wire generates a Faraday voltage proportional to the velocity which we detect. The width of the resonance provides a measure of the damping of the wire motion. In superfluid ^{3}He-*B* at low wire velocities, the damping has a temperature-independent intrinsic component from internal losses in the wire plus a temperature-dependent component from the thermal quasiparticle gas. At our low temperatures the quasiparticle excitations in the *B* phase are highly ballistic, and the thermal damping arises from those excitations scattered normally by the wire. This leads to a damping which is proportional to the quasiparticle density with a temperature dependence given by the Boltzmann factor $\exp(-\Delta/kT)$. The thermal damping is greatly enhanced by Andreev scattering from the superfluid backflow around the wire. In a superfluid flow of velocity $\mathbf{v}$, the quasiparticle dispersion curve becomes tilted by an energy $\mathbf{p} \cdot \mathbf{v}$. A flow gradient therefore leads to Andreev scattering of low energy excitations. In the case of a vibrating wire, the backflow predominantly Andreev scatters quasiholes incident on the front of the wire and quasiparticles incident on the rear leading to an enhancement of the damping by several orders of magnitude [7].

Above a critical velocity $v_c = v_L/3$, where v_L is the Landau critical velocity Δ/p_F, the moving wire can also break Cooper pairs leading to a very rapid rise in the damping [8]. The quasiparticle excitations released from the broken pairs are emitted in a rather narrow beam along the axis of the wire motion [9]. Furthermore, from recent measurements we know that at velocities a little below v_c vortex lines are also produced, presumably at excrescences on the wire surface [3].

In the present experiments we measure the thermal damping of the detector wire, driven at low velocity, while we drive the generator wire above the pair-breaking velocity. The detector wire is maintained on resonance so that we may deduce the damping Δf_2 from the detector output voltage. The damping is recorded as a function of the velocity v_g of the generator wire inferred from the generator signal. The measurements are then repeated at various temperatures.

There are two principal features seen in the response of the detector. First, over a narrow range of generator wire velocities slightly above $v_L/3$, we see an increase in damping caused by the excitation beam emitted by the generator [9]. This effect is most noticeable at the lowest temperatures where the background thermal excitation density is

 0031-9007/01/86(2)/244(4)$15.00

negligible. However, a surprising new effect occurs when the velocity of the generator is increased further; the damping of the detector begins to *fall* sharply. In other words, when we move the generator faster, the damping from thermal excitations on the detector falls below the level when the generator is stationary. This remarkable behavior is the subject of this Letter.

In Fig. 1 we show the detector damping (in terms of its inferred resonant width, Δf_2) as a function of time while we apply excitation current to the generator wire. The data were taken at a temperature of $0.185T_c$ where the thermal damping on the detector is 300 times larger than the intrinsic value. The velocities for the generator have a systematic uncertainty of around 10% arising from the nonideal geometry of the wire loop. Clearly, despite the extra quasiparticle flux emitted from the generator, the damping on the detector (from all sources) *decreases*. Thus there must be a reduction of the damping from the gas of thermal excitations. This reduction in the thermal damping implies that the flux of thermal quasiparticles reaching the detector is diminished. Since quasiparticle-quasiparticle scattering is negligible at these temperatures we are forced to conclude that the screening of the detector from thermal quasiparticles must be due to Andreev scattering from an additional flow field generated by the generator, that is to say, from turbulence.

We deduce the fraction of the thermal quasiparticle flux screened from the detector wire as follows. The damping of the detector (after we subtract the small intrinsic contribution) is proportional to the incident quasiparticle flux on the wire. At our base temperature where the background density of thermal quasiparticles is essentially zero, the increase in the detector damping as a function of the generator wire velocity $\delta\Delta f_2^0(v)$ arises entirely from those quasiparticles emitted in the pair-breaking beam. This contribution we assume to be temperature independent.

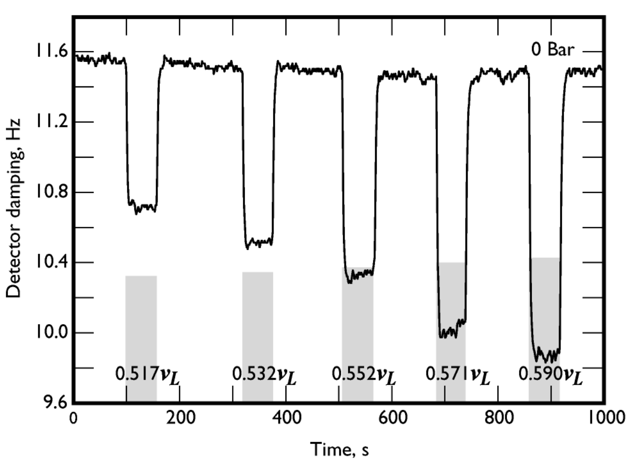

FIG. 1. The damping on the detector wire as a function of time while a series of drives are applied to the generator wire during the periods indicated by the hatching. For each period the peak generator wire velocity is shown as a fraction of the Landau critical velocity.

At the higher temperatures, the corresponding change in the damping $\delta\Delta f_2^T(v)$ has an extra negative contribution from the screening of the thermal quasiparticles, given by $\delta\Delta f_2^T(v) - \delta\Delta f_2^0(v)$. The fractional change in the thermal quasiparticle flux incident on the detector is thus $[\delta\Delta f_2^T(v) - \delta\Delta f_2^0(v)]/\Delta f_2^T(0)$, where $\Delta f_2^T(0)$ is the detector damping when the generator is not driven. This is plotted in Fig. 2A as a function of the peak generator wire velocity scaled by the Landau critical velocity v_L. Experimental points are shown for a range of temperatures between $0.17T_c$ and $0.26T_c$ and for two different cell pressures, 0 and 5 bars. The pair-breaking critical velocity of the generator wire is found to be $v_L/3$ as expected [8] and the fractional screening rises quite sharply for generator wire velocities exceeding $0.4v_L$. The rise is sharper at the higher pressure reaching a maximum value of around 20%, with the screening then falling towards higher temperatures.

To understand the data of Fig. 2A we note that a quasiparticle excitation traveling through a region of changing superflow $\mathbf{v}(\mathbf{r})$ experiences a varying effective potential

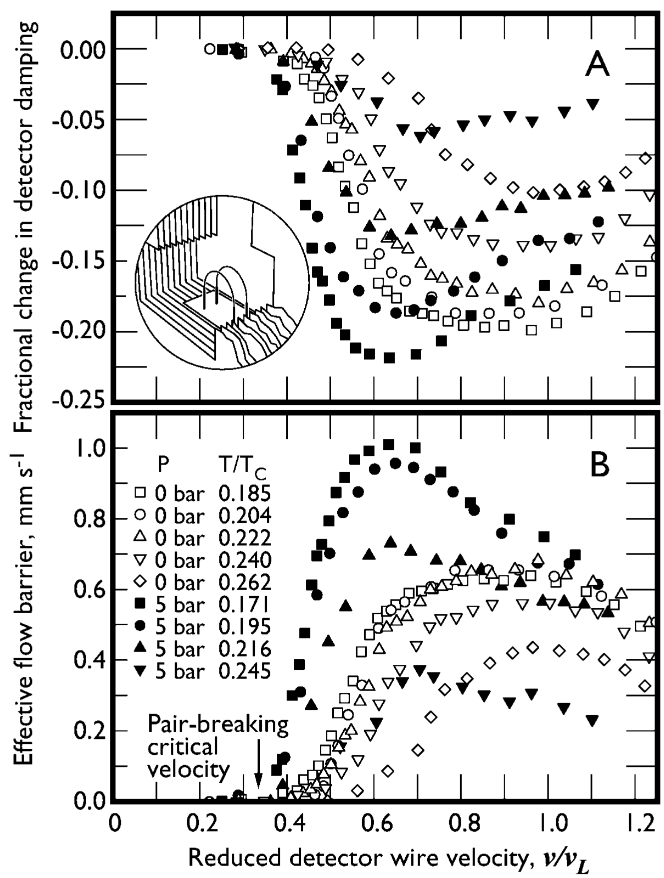

FIG. 2. (A) The fractional change in thermal damping of the detector wire as a function of the generator wire peak velocity normalized to the Landau velocity v_L. (B) The effective flow barrier presented by the turbulence to quasiparticle excitations incident on the detector wire as a function of generator wire peak velocity. Inset: the inner part of the cell showing the open volume in the sinter plates and the two vibrating wires.

energy $\mathbf{p} \cdot \mathbf{v}(\mathbf{r})$ arising from the distortion of the excitation dispersion curve by the flow field. We may picture a flow field from vortices near the wire as shown schematically in Fig. 3A. The tangle of vortices therefore produces a potential made up of a sequence of overlapping peaks as shown in Fig. 3B (as viewed from the wire). For incoming excitations with energies less than the maximum effective potential along the trajectory, one flavor (either quasiparticle or quasihole depending on the direction of the velocity field) will be Andreev reflected. The other flavor can reach the wire and be normally reflected but then finds no outgoing states and is returned to the wire and can escape only after a subsequent flavor-switching Andreev process. Either way, excitations with energies less than the peak energies along their paths as illustrated cannot exchange momentum with the wire. As far as the mechanics of the wire is concerned this has the effect of truncating the distribution of thermal excitations which participate in damping the wire motion to those with energies above the maximum peak energy along the trajectory. We may model the tangle as presenting an average energy barrier $p_F v_b$ to the thermal quasiparticles approaching the detector wire. The flow barrier v_b represents the angular averaged maximum flow present along the excitation trajectories crossing the tangle. Within this simple model, the effect of the flow barrier on the damping of the detector wire is equivalent to that of an enhanced energy gap.

In the absence of vortices the damping is proportional to the Boltzmann factor $\exp(-\Delta/kT)$ so we model the effect of the vortices by replacing this factor by $\exp[-(\Delta + p_F v_b)/kT]$. The fractional change in the thermal damping plotted in Fig. 2A is then given by $f = 1 - \exp[-(p_F v_b)/kT]$. The effective flow barriers v_b obtained from the data of Fig. 2A using this expression are presented in Fig. 2B. The flow barrier is seen to be somewhat lower at the 0 bar with very little temperature dependence below $0.22T_c$ and decreasing at higher temperatures. The number of vortices required to produce such an effective barrier will depend both on the spatial extent of the tangle and the vortex density within it. However, to put into context the deduced magnitude of the barrier which corresponds to a flow of order 1 mm/s, we note that the flow around an isolated vortex reaches this level at a radius of approximately 10 μm. This value provides a rough limit that the mean vortex separation in the tangle must be on a scale greater than 20 μm.

We also observe transient behavior in the response of the detector to the turbulence. In Fig. 4 we plot the thermal damping on the detector as a function of time while driving the generator at high velocities. The temperature

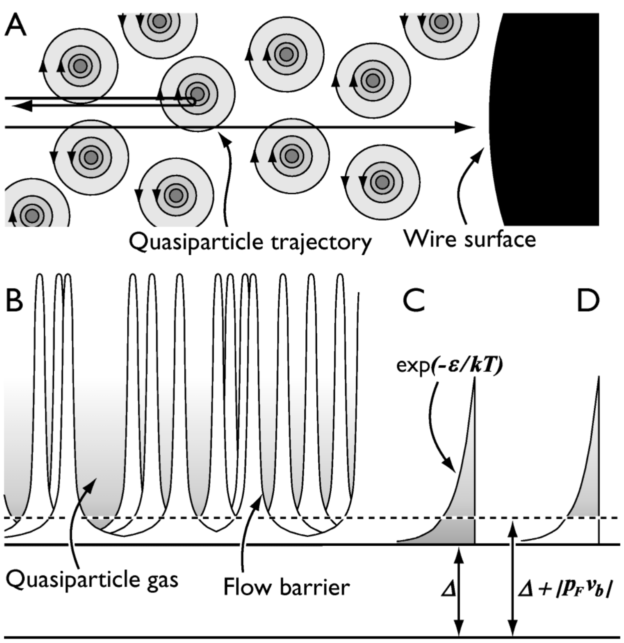

FIG. 3. (A) A schematic map of the velocity field along the trajectory of an excitation reaching the wire surface. (B) The effective flow barrier placed in the way of a flux of quasiparticle and quasihole excitations approaching the viewer. Each vortex contributes a peak to the total flow-dependent potential barrier presented by the tangle (see text). The mean barrier height of $p_F v_b$ represents an angular average over the trajectories of all incoming and outgoing excitations. (C) The bulk thermal distribution of excitations. (D) The mean distribution of excitations which can penetrate the tangle to the wire, be normally scattered, and then escape again to the bulk.

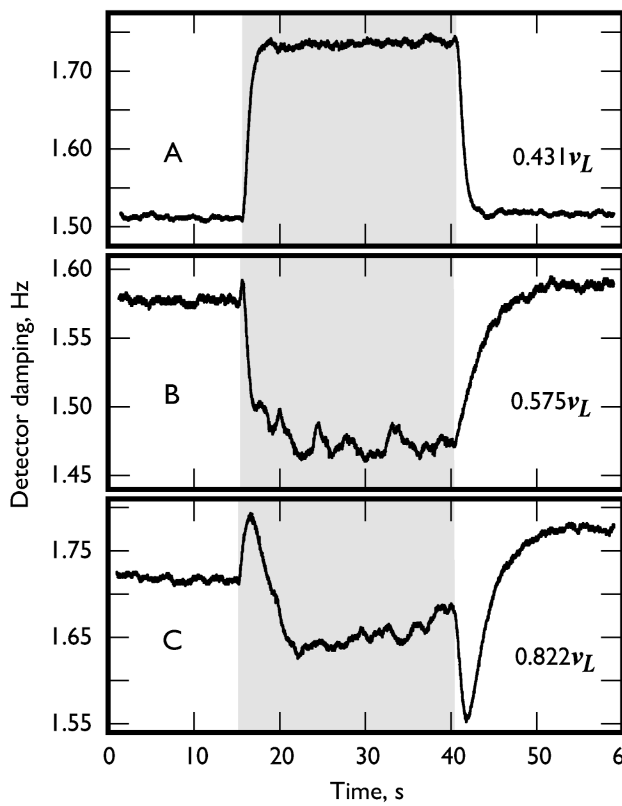

FIG. 4. The damping on the detector wire as a function of time as the generator wire is driven at three different peak velocities at $T = 0.153T_c$ at 0 bar pressure. The shaded region indicates the period when the generator wire drive was on. The appropriate peak generator wire velocity is shown in the figure.

here is sufficiently low that the pair-breaking beam from the generator provides a significant contribution to the detector damping. Figure 4A shows the response when the generator is driven at $0.431v_L$, a velocity at which the turbulence is just becoming visible on the higher temperature data. Here the response is dominated by the pair-breaking beam and a relatively rapid increase in the damping is observed with a time constant limited by the measuring circuit. Figure 4B shows the response when the generator wire is driven at $0.575v_L$, where the pair-breaking beam contribution is still very significant but the turbulence is now sufficient to give a net decrease in damping. The small transient increase after the generator wire is switched on indicates that the turbulence is not established instantaneously (the pair-breaking beam contribution is effectively instantaneous on this time scale). After the initial transient, the detector damping decreases quite rapidly at first and then more gradually over a period of several seconds. The response is also seen to become noisy on a time scale of order 1 s. On switching off the generator wire, the detector damping recovers much more slowly with a time constant of order 4 s. The response of the detector to higher generator wire velocities, as shown in Fig. 4C, still shows a decrease in damping. However, there is now transient cooling immediately after switching off the generator, owing to the immediate loss of the pair-breaking beam contribution.

The increased noise in the detector output in the presence of turbulence presumably reflects the continually changing distribution of vortices in the detector wire's vicinity. The 1 s time scale of this noise is reasonable, given that vortex loops with diameters of order 10 μm will travel at velocities of order 1 mm/s and that the turbulent region must have a spatial extent of scale 1 mm, comparable to the length and separation of the wires.

The decay time of the screening effect of the turbulence on the detector damping when the generator is switched off is quite insensitive to the generator wire velocity, temperature and pressure, always being of order 3 to 4 s. With the current experiment we cannot tell whether this reflects the intrinsic decay of the vorticity with time or the spatial evolution of the vortex tangle taking it away from the detector. However, the growth time of the screening becomes very similar to the decay time at high temperatures, suggesting that the spatial evolution of the vortex tangle is responsible.
At lower temperatures where the pair-breaking beam contribution is much more significant, the initial growth of the vortex screening is much more rapid and we speculate that here the quasiparticle wind from the generator beam may carry the vortex tangle towards the detector. At higher temperatures, where compared to the thermal background the quasiparticle flux in the beam is small, one would not expect it to have a significant effect on the tangle evolution.

In conclusion, we have created and observed turbulence in superfluid ^{3}He-B with vibrating-wire resonators. In this experiment we are really making a movie using the illumination of the surrounding thermal quasiparticle "light" and observing the shadows thrown by the vortex tangle on the detector wire. At present the camera records only one pixel covering a large spatial extent, the active length of the wire. However, even with this crude "image" the fluctuations of the shadows can be seen, showing the time evolution of the turbulence on a time scale of order 1 s.

These preliminary measurements indicate several ways in which more specific properties of superfluid turbulence may be studied directly. Detector wires covering smaller spatial extents either singly or in arrays should enable us to make images which might resolve the influence of individual vortices. We could then look directly at the processes of vortex dynamics and decay on the vortex scale. It is an interesting thought that in some sense superfluid turbulence provides an alternative to aerogel in adding spatial disorder to the superfluid, with an Andreev rather than a normal scattering mechanism determining the mean free paths of the excitation gas.

We thank I. E. Miller and M. G. Ward for their technical backup, and the U.K. EPSRC for financial support.

[1] S. R. Stalp, L. Skrbek, and R. J. Donnelly, Phys. Rev. Lett. **82**, 4831 (1999).
[2] C. Bäuerle, Yu. M. Bunkov, S. N. Fisher, H. Godfrin, and G. R. Pickett, Nature (London) **382**, 322 (1996).
[3] D. I. Bradley, Phys. Rev. Lett. **84**, 1252 (2000).
[4] See, for example, V. M. H. Ruutu, Ü. Parts, J. H. Koivuniemi, N. B. Kopnin, and M. Krusius, J. Low Temp. Phys. **107**, 93 (1997).
[5] C. A. M. Castelijns, K. F. Coates, A. M. Guénault, S. G. Mussett, and G. R. Pickett, Phys. Rev. Lett. **56**, 69 (1986).
[6] See, for example, G. R. Pickett, Rep. Prog. Phys. **51**, 1295 (1988).
[7] S. N. Fisher, A. M. Guénault, C. J. Kennedy, and G. R. Pickett, Phys. Rev. Lett. **63**, 2566 (1989).
[8] C. J. Lambert, Physica (Amsterdam) **165B–166B**, 653 (1990).
[9] S. N. Fisher, A. M. Guénault, C. J. Kennedy, and G. R. Pickett, Phys. Rev. Lett. **69**, 1073 (1992).